ELSEVIER

Journal of Hydrology 165 (1995) 261–281

Journal of Hydrology

[2]

Analysis of a model for contaminant transport in fractured media in the presence of colloids

Assem Abdel-Salam, Constantinos V. Chrysikopoulos*

Department of Civil and Environmental Engineering, University of California, Irvine, CA 92717, USA

Received 18 September 1993; revision accepted 15 June 1994

Abstract

A mathematical model has been developed to study the cotransport of contaminants with colloids in saturated rock fractures. The contaminant is assumed to decay, and sorb on to fracture surfaces and on to colloidal particles, as well as to diffuse into the rock matrix; whereas, colloids are envisioned to deposit irreversibly on to fracture surfaces without penetration into the rock matrix. The governing one-dimensional equations describing the contaminant and the colloid transport in the fracture, colloid deposition on to fracture surfaces, and contaminant diffusion into the rock matrix are coupled. This coupling is accomplished by assuming that the amount of contaminant mass captured by colloidal particles in solution and the amount captured by deposited colloids on fracture surfaces are described by modified Freundlich reversible equilibrium sorption relationships, and that mass transport by diffusion into the rock matrix is a first-order process. The contaminant sorption on to fracture surfaces is described by a linear equilibrium sorption isotherm, while the deposition of colloids is incorporated into the model as a first-order process. The resulting coupled contaminant transport non-linear equation is solved numerically with the fully implicit finite difference method. The constant concentration as well as the constant flux boundary conditions have been considered. The impact of the presence of colloids on contaminant transport is examined. According to model simulations the results show that, depending on the conditions of the physical system considered, colloids can increase or decrease the mobility of contaminants.

1. Introduction

Hazardous wastes, especially radioactive materials, are disposed of in canisters that are usually buried in deep fractured, low-permeability bedrocks. The possible leakage of these canisters has stimulated a great deal of interest in studying contaminant

* Corresponding author.

SSDI 0022-1694(94)02557-R

Notation

a	curve fitting parameter for the modified Freundlich adsorption isotherm
b	fracture aperture (L)
c	contaminant concentration in the fracture ($M L^{-3}$)
c_m	contaminant concentration in the rock matrix ($M L^{-3}$)
c_0	source contaminant concentration ($M L^{-3}$)
c^*	contaminant concentration adsorbed on to fracture surfaces ($M L^{-2}$)
c_m^*	contaminant concentration adsborbed inside the rock matrix ($M M^{-1}$)
d	curve fitting parameter for the modified Freundlich adsorption isotherm
d_p	colloidal particle diameter (L)
D	hydrodynamic dispersion coefficient ($L^2 T^{-1}$)
$\mathscr{D}_m$	effective diffusion coefficient in the rock matrix ($L^2 T^{-1}$)
K_f	partition coefficient for contaminant sorption on to fracture surfaces (L)
K_m	contaminant partition coefficient in the rock matrix ($L^3 M^{-1}$)
K_n	partition coefficient for contaminant sorption on to suspended colloids ($(M M^{-1})^{1-a}$)
K_{n^*}	partition coefficient for contaminant sorption on to deposited colloids ($(M M^{-1})^{1-d} L^d$)
n	colloid concentration in the liquid phase ($M L^{-3}$)
n_0	source colloid concentration ($M L^{-3}$)
n^*	colloid concentration deposited on to fracture surfaces ($M L^{-2}$)
n_{max}^*	maximum deposited colloid concentration on fracture surfaces ($M L^{-2}$)
N_{max}^*	maximum number of deposited colloids per unit fracture surface area
q^*	diffusive mass flux normal to the fracture–matrix interface ($M L^{-2} T$)
R	retardation factor in the fracture
R_m	retardation factor in the rock matrix
s	contaminant concentration adsorbed on to colloids in the liquid phase ($M M^{-1}$)
s_0	source solid-phase contaminant concentration on to suspended colloids ($M M^{-1}$)
s^*	contaminant concentration adsorbed on to deposited colloids ($M M^{-1}$)
t	time (T)
U	average interstitial velocity in the fracture ($L T^{-1}$)
x	coordinate along the fracture axis (L)
z	coordinate perpendicular to the fracture axis (L)

Greek Letters

α	area blocked by each deposited particle (L^2)
ϵ	fraction of the fracture surface covered by colloids
θ	porosity of the rock matrix
κ	colloid deposition coefficient (L)
λ	first-order decay coefficient (T^{-1})
ρ_b	bulk density of the rock matrix ($M L^{-3}$)
ρ_p	colloidal particle density ($M L^{-3}$)

migration in fractured media, and in investigating the capacity of natural barriers to slow down the movement of leaked contaminants (e.g. Neretnieks et al., 1982; Abelin, 1986; Raven et al., 1988; Krishnamoorthy, 1992).

The basic constructive unit in fractured media is a single fracture. For example, a single fracture is often used to represent a medium consisting of a series of parallel fractures (Van der Lee et al., 1992). Thus, in order to study contaminant transport in fractured networks, it is important to understand the transport mechanisms in a single fracture. Various investigations have focused on modeling flow and contaminant transport in a single fracture (Neuzil and Tracy, 1981; Neretnieks, 1983;

Novakowski et al., 1985; Tsang and Tsang, 1987; Moreno et al., 1988; Shapiro and Nicholas, 1989; Johns and Roberts, 1991, to mention a few representative studies). A typical idealization of a natural single fracture is a pair of parallel plates separated by an average aperture. Surrounding the two fracture plates is the host rock matrix which, for all practical purposes, can be treated as a very tight porous medium.

The two major retention mechanisms for contaminants transported in fractured media are diffusion and sorption. Diffusion into surrounding rock matrix microfissures occurs in response to fracture rock-matrix concentration gradients and may be significant in diluting the concentration of contaminants (Skagius and Neretnieks, 1986). For example, in two safety analyses in fractured rocks, namely KBS-3 (1983) and NAGRA (Project Gewahr) (1985), the uptake of radionuclides into the rock matrix is proven to be the most important dilution mechanism. Matrix diffusion rates are dependent upon the interstitial fluid velocity in the fracture, and the contact area between the flowing fluid and the rock matrix (Abelin, 1986). Sorption reactions (ion exchange, physical and chemical sorption) occur at fracture surfaces. The magnitude of contaminant retardation is proportional to the surface area in contact with the flowing liquid, surface roughness, and the interstitial fluid velocity (Abelin, 1986). Furthermore, contaminants diffused into the rock matrix may sorb on to the solid surfaces of microfissures.

Recent experimental and field studies indicate that contaminants can migrate not only as dissolved species in the liquid phase, but also adsorbed on to the surface of suspended colloid particles (e.g. Torok et al., 1990; Buddemeier and Hunt, 1988; Chiou et al., 1986). Therefore, colloid particles serve as carriers for contaminants and may significantly influence the net rate of contaminant migration. Puls and Powell (1992) concluded from laboratory experiments that iron oxide colloids may be mobile to a significant extent, and under some conditions these colloids may be transported faster than conservative tracers. At the Nevada test site, radionuclide analyses for detonation-cavity samples indicated that substantial fractions of selected nuclides are associated with colloid-sized particles (Buddemeier and Hunt, 1988). Rapid transport of bacterial colloids, relative to conservative tracers, was observed in a field experiment in crystalline fractured rocks (Champ and Schroeter, 1988). At two separate sites at Los Alamos, New Mexico, plutonium and americium were detected at distances much further than the distances predicted by conventional techniques (Corapcioglu and Jiang, 1993). Since colloids have high surface area per unit mass, relatively more contaminant will be attached to colloids than to solid surfaces (McDowell-Boyer et al., 1986; Toran and Palumbo, 1992). Furthermore, colloids are more accessible to contaminants than fracture surfaces.

Colloids are very fine particles that typically range in diameter between 10^{-3} and 1 μm (Buddemeier and Hunt, 1988). Several types of organic as well as inorganic colloids may be present in the subsurface environment. The most frequently encountered colloids are humic substances, bacteria, viruses, clay minerals and macromolecules (Mills et al., 1991; Moulin and Ouzounian, 1992). Colloids may be introduced to or formed in groundwater, for instance, as a result of well drilling operations, leachates from the vadose zone, and dissolution of inorganic cementing agents that bind colloidal-sized materials to solid surfaces (McCarthy and Zachara,

1989). Moreover, well pumping, rising water tables, and replacement of saline water by fresh water may initiate particle mobilization (Corapcioglu and Jiang, 1993). Colloids may also be generated when ionic metal species are at concentrations above their solubility limit (Buddemeier and Hunt, 1988). Colloids are found in subsurface waters under various geochemical conditions with concentrations ranging from a few milligrams per liter to a few hundred milligrams per liter (Moulin and Ouzounian, 1992). For instance, a high particle concentration has been found in granitic rock fractures at the Nevada test site (63 mg l^{-1}) and in Switzerland (10^{10} particles l^{-1}) (Buddemeier and Hunt, 1988; Mills et al., 1991).

Colloids are subjected to sorption reactions with surrounding fracture surfaces. The adsorption process of colloids on to solid surfaces is conventionally termed as filtration or deposition, while colloid desorption is known as detachment. A field experiment in crystalline rock fractures has demonstrated that the primary removal mechanism of bacterial and non-reactive colloids from a bulk solution is by deposition (Champ and Schroeter, 1988). Deposition of colloids is generally affected by Brownian motion, the repulsive electric double layer, attractive van der Waals forces, and solution chemistry (Mills et al., 1991). These mechanisms influence the stability of colloidal particles in solution and the interactions between particles and fracture surfaces. Particle deposition is also affected by whether fracture surfaces are clean or deposition occurs on previously deposited particles (De Marsily, 1986). Comprehensive compilations of particle deposition mechanisms have been presented by McDowell-Boyer et al. (1986), and McCarthy and Zachara (1989). Detachment of colloids is not expected in fractured rocks where flow velocities are low. Bowen and Epstein (1979) have shown experimentally that the rate of release of deposited colloids from a smooth parallel-plate channel is negligible. The penetration of colloids into the rock matrix is not highly likely because of their weak diffusivities. Bradbury and Green (1986) found that particles in the size range of 0.091–0.312 μm cannot penetrate a crystalline rock matrix with 0.14 μm microfissures. Nevertheless, the possibility of colloids diffusing into the rock matrix can not be eliminated given that colloids range in size between 10^{-3} and 1 μm; whereas, the size of rock-matrix microfissures ranges between 0.01 and 10 μm (Birgersson and Neretnieks, 1982).

Several researchers have attempted modeling the transport of colloids and colloid-facilitated contaminant transport in subsurface environments. Corapcioglu and Haridas (1985) developed a mathematical model describing the transport of microbial pollutants in porous media in the presence of a nutrient. Mills et al. (1991) presented a model to evaluate the significance of colloids on the mobility of metals in porous media. Van der Lee et al. (1992) modeled uranium transport in fractured media to investigate the case of colloid-forming uranium at concentration levels above uranium solubility limit. Corapcioglu and Jiang (1993) derived a model for colloid-facilitated transport in porous media and examined both cases of equilibrium and kinetic contaminant sorption on tc colloids. Smith and Degueldre (1993) modeled the transport of a radioactive material in the presence of colloids in a single fracture; however, their model does not account for the progressive reduction in contaminant diffusion into the rock matrix and sorption on to fracture surfaces owing to deposition of colloids. Moreover, their model assumes a uniform and steady

colloidal distribution in the fracture, and neglects all possible interactions of the contaminant with deposited colloids.

In this paper a model describing contaminant transport in the presence of colloids within a single fracture idealized as two parallel plates is presented. The model accounts for contaminant sorption on to fracture surfaces, contaminant diffusion into the rock matrix in conjunction with matrix sorption, transport of colloids in the fracture, deposition of colloids on to fracture surfaces, and contaminant sorption on to suspended as well as deposited colloids. Furthermore, the reduction in matrix diffusion and fracture sorption owing to deposition of colloids is also accounted for. Two one-dimensional equations, one for colloid transport in a fracture coupled with colloid deposition on to fracture surfaces, and the other for contaminant diffusion into the rock matrix are used in the development of the model. The solution to the system of coupled partial differential equations is obtained numerically using the fully implicit finite difference method for a semi-infinite fracture, subject to constant concentration as well as constant flux inlet boundary conditions. The numerical code is verified against an analytical solution for the simple case where no colloids are present. Model simulations are performed to investigate the impact of the model parameters on the spatial and temporal evolution of the contaminant.

2. Model development

The one-dimensional contaminant transport in a semi-infinite fracture in the presence of colloids, assuming that the contaminant may decay and sorb on to colloids as well as on to fracture surfaces, diffuse into the rock matrix; while, colloids may deposit on to fracture surfaces but may not penetrate the rock matrix (see Fig. 1), is governed by the following partial differential equation

(Accumulation = Dispersion − Advection − Matrix diffusion − Decay)

$$\frac{\partial}{\partial t}\left[c(t,x)+\frac{2(1-\epsilon)}{b}c^*(t,x)+n(t,x)s(t,x)+\frac{2}{b}n^*(t,x)s^*(t,x)\right]$$

$$=D\frac{\partial^2}{\partial x^2}[c(t,x)+n(t,x)s(t,x)]-U\frac{\partial}{\partial x}[c(t,x)+n(t,x)s(t,x)]$$

$$-\frac{2(1-\epsilon)}{b}q^*-\lambda\left[c(t,x)+\frac{2(1-\epsilon)}{b}c^*(t,x)+n(t,x)s(t,x)+\frac{2}{b}n^*(t,x)s^*(t,x)\right] \tag{1}$$

where c is the contaminant concentration in the fracture; t is time; x is the distance along the fracture axis; D is the hydrodynamic dispersion coefficient; n is the concentration of colloids suspended in the liquid phase; s is the contaminant concentration adsorbed on to suspended colloids in the liquid phase, expressed as mass of contaminant per mass of colloids; U is the average interstitial velocity; b is the fracture aperture; ϵ is the fraction of the fracture surface covered by colloids, which is time and space dependent; n^* is the concentration of colloids deposited on to

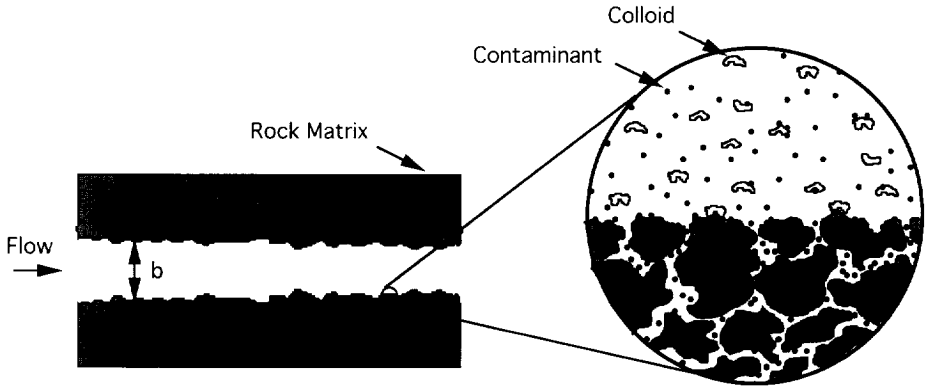

Fig. 1. Schematic illustration of contaminant transport in a fracture in the presence of colloids. Contaminants can sorb on to colloids as well as on to the fracture surfaces and may diffuse into the rock matrix. Colloids deposit on to the fracture surfaces but do not penetrate the rock matrix.

fracture surfaces, expressed as mass of colloids per unit area of the fracture surface; c^* is the contaminant concentration adsorbed on to fracture surfaces, expressed as mass of contaminant per unit area of fracture surface; s^* is the contaminant concentration adsorbed on to deposited colloids, expressed as mass of contaminant per mass of deposited colloids; λ is a first-order decay coefficient; and q^* is the diffusive mass flux of the contaminant in a direction perpendicular to the fracture–matrix interface. The governing transport equation (1) has been derived from a mass balance over a representative fracture volume. The term $n(t,x)s(t,x)$ represents the contaminant adsorbed on suspended colloids, while the term $(2/b)\partial[n^*(t,x)s^*(t,x)]/\partial t$ represents the deposition of colloidal particles with sorbed contaminant on their surfaces in conjunction with contaminant sorption on to deposited particles $[n^*(t,x)s^*(t,x) = (1-\epsilon)n^*(t,x)s^*(t,x) + \epsilon n^*(t,x)s^*(t,x)]$. It should be noted that in the derivation of the governing transport equation we have assumed that contaminant sorption on to a colloidal particle does not alter its hydrodynamic and deposition mechanisms. The hydrodynamic dispersion coefficient of colloidal particles is the sum of mechanical dispersion and Brownian diffusion, while for the case of molecular size contaminants it is the sum of mechanical dispersion and molecular diffusion. Generally, mechanical dispersion dominates Brownian diffusion and molecular diffusion. Therefore, the same hydrodynamic dispersion coefficient is used for both the contaminant and colloids. The velocity distribution across the two plates of a fracture is parabolic (Poiseuille flow) with zero magnitude at the fracture surfaces and a maximum magnitude of 1.5 times the average velocity midway between the two plates. However, in this work the velocity across the fracture width is assumed to be constant and equal to its vertically averaged magnitude.

Contaminant sorption on to fracture surfaces is assumed to be governed by the following linear reversible equilibrium isotherm

$$c^*(t,x) = K_f c(t,x) \tag{2}$$

where K_f is the partition coefficient for contaminant sorption on to fracture surfaces. It should be noted that contaminant sorption on to fracture surfaces is influenced by

the available fracture surface-area for sorption, which is a function of the deposited colloid concentration. The reduction in contaminant sorption on to fracture surfaces, and contaminant diffusion into the rock matrix due to colloid deposition is accounted for by adjusting the value of ϵ, which ranges from a lower limit of zero for the case of no colloid deposition to an upper limit of one for a complete monolayer coverage of the fracture surface ($0 \leqslant \epsilon \leqslant 1$). Summers and Roberts (1988), and McKinley and Jenne (1991) suggest the following modified Freundlich reversible equilibrium isotherm for contaminant sorption on to colloids

$$s(t,x) = K_n \left[\frac{c(t,x)}{n(t,x)}\right]^a \tag{3}$$

where K_n is the partition coefficient for contaminant sorption on to suspended colloids; and a is the isotherm fitting parameter. A similar modified Freundlich isotherm is employed for contaminant sorption on to deposited colloids

$$s^*(t,x) = K_{n^*} \left[\frac{c(t,x)}{n^*(t,x)}\right]^d \tag{4}$$

where K_{n^*} is the partition coefficient for contaminant sorption on to deposited colloids; and d is the isotherm fitting parameter. It should be noted that the partition coefficients K_f, K_n, and K_{n^*} may or may not be independent from each other; however, this information is not presently available in the literature. The diffusive mass flux normal to the fracture–matrix interface is expressed by Fick's first law as (Tang et al., 1981)

$$q^* = -\theta \mathscr{D}_m \frac{\partial c_m(t,x)}{\partial z}\Big|_{z=b/2} \tag{5}$$

where θ is the porosity of the rock matrix; $\mathscr{D}_m$ is the effective diffusion coefficient in the rock matrix; c_m is the contaminant concentration in the rock matrix; and z is the distance perpendicular to the fracture axis. Substituting Eqs. (2)–(5) into Eq. (1) yields the following equation for contaminant transport in a fracture

$$\begin{aligned}
&\frac{\partial c}{\partial t}\left[1 + \frac{2(1-\epsilon)K_f}{b} + aK_n\left(\frac{c}{n}\right)^{a-1} + \frac{2dK_{n^*}}{b}\left(\frac{c}{n^*}\right)^{d-1}\right] \\
&= aK_nD\frac{\partial^2 c}{\partial x^2}\left[\left(\frac{c}{n}\right)^{a-1} + \frac{1}{aK_n}\right] + aK_n\frac{\partial c}{\partial x}\left\{\left(\frac{c}{n}\right)^{a-1}\left[\frac{2(1-a)D}{n}\frac{\partial n}{\partial x} - U\right]\right. \\
&\quad \left. + \frac{(a-1)D}{n}\left(\frac{c}{n}\right)^{a-2}\frac{\partial c}{\partial x} - \frac{U}{aK_n}\right\} + (a-1)K_n\left(\frac{c}{n}\right)^a\left[\frac{\partial n}{\partial t} + U\frac{\partial n}{\partial x} - D\frac{\partial^2 n}{\partial x^2}\right. \\
&\quad \left. + \frac{aD}{n}\left(\frac{\partial n}{\partial x}\right)^2\right] - \frac{2(1-d)K_{n^*}}{b}\left(\frac{c}{n^*}\right)^d\frac{\partial n^*}{\partial t} + \frac{2(1-\epsilon)\theta\mathscr{D}_m}{b}\frac{\partial c_m}{\partial z}\Big|_{z=b/2} \\
&\quad - \lambda\left\{c\left[1 + \frac{2(1-\epsilon)K_f}{b}\right] + \frac{2K_{n^*}}{b}n^*\left(\frac{c}{n^*}\right)^d + K_n n\left(\frac{c}{n}\right)^a\right\}
\end{aligned} \tag{6}$$

In order to solve the preceding contaminant transport partial differential equation, it is necessary to provide mathematical expressions for the time- and space-dependent colloid concentration in the fracture (both in the liquid phase, n, and deposited on to fracture surfaces, n^*), and contaminant concentration in the rock matrix. Appropriate expressions for $n(t,x)$ and $n^*(t,x)$ are presented in the next section. The expression for $c_m(t,x,z)$ can be obtained from the following one-dimensional partial differential equation governing contaminant diffusion in a direction perpendicular to the fracture axis, assuming that the interstitial liquid in the rock matrix is stationary and the contaminant undergoes decay and sorption on to the rock matrix (Tang et al., 1981)

$$\frac{\partial c_m(t,x,z)}{\partial t} = \frac{\mathscr{D}_m}{R_m}\frac{\partial^2 c_m(t,x,z)}{\partial z^2} - \lambda c_m(t,x,z) \tag{7}$$

where R_m is the retardation factor in the rock matrix defined as

$$R_m = 1 + \frac{\rho_b K_m}{\theta} \tag{8}$$

which implies that contaminant sorption on to the rock-matrix solid-surfaces is described by a linear reversible equilibrium isotherm; ρ_b is the bulk density of the rock matrix; and $K_m = c_m^*/c_m$ is the contaminant partition coefficient in the rock matrix defined as the mass of contaminant adsorbed per unit mass of solid rock matrix (c_m^*) divided by the contaminant concentration in the rock matrix (c_m). The following initial and boundary conditions are employed

$$c(0,x) = 0 \tag{9}$$

$$c(t,0) = c_0 \tag{10a}$$

$$-D\frac{\partial c(t,0)}{\partial x} + Uc(t,0) = Uc_0 \tag{10b}$$

$$\frac{\partial c(t,\infty)}{\partial x} = 0 \tag{11}$$

$$c_m(0,x,z) = 0 \tag{12a}$$

$$c_m(t,x,b/2) = c(t,x) \tag{12b}$$

$$\frac{\partial c_m(t,x,\infty)}{\partial z} = 0 \tag{12c}$$

where c_0 is the contaminant concentration at the source. It should be noted that for a given problem either Eq. (10a) or Eq. (10b) is used for constant concentration and constant flux boundary condition cases, respectively, but not both. Furthermore, we assume that the contaminant and colloids are introduced simultaneously at the inlet boundary, and that c_0 and n_0 are in equilibrium at the boundary. This implies that a solid-phase contaminant concentration adsorbed on to suspended colloids, s_0, is also introduced at the source.

The solution to the non-linear equation (6) coupled with Eq. (7) is obtained numerically by the fully implicit finite difference method, as outlined by Strikwerda (1989). A two-point backward difference approximation for the time derivative and a central difference approximation for the spatial derivatives are employed. The resulting approximation is second-order accurate. For the case of constant flux boundary condition (10b), a second-order, one-sided finite difference approximation is employed (Strikwerda, 1989). Since Eq. (6) is non-linear, the resulting set of finite difference algebraic equations is also non-linear. Therefore, the Newton–Raphson method, as presented in Huyakorn and Pinder (1983) and Kahaner et al. (1989), is employed to linearize the algebraic finite difference equations. Moreover, the Newton–Raphson linearized equations are solved by the banded LU decomposition matrix solver algorithm (Press et al., 1992).

3. Analytical solutions for colloid transport

The partial differential equation describing one-dimensional colloid transport in a single fracture, allowing for irreversible colloid deposition on to fracture surfaces, derived from mass balance considerations, is given by

$$\frac{\partial n(t,x)}{\partial t} = D\frac{\partial^2 n(t,x)}{\partial x^2} - U\frac{\partial n(t,x)}{\partial x} - \frac{2}{b}\frac{\partial n^*(t,x)}{\partial t} \tag{13}$$

where the last term in the preceding equation represents the mass flux of colloids on to fracture surfaces which is restricted as follows

$$\frac{\partial n^*(t,x)}{\partial t} = \begin{cases} \dfrac{\kappa U}{b} n(t,x), & n^* < n^*_{\max} \\ 0, & n^* \geqslant n^*_{\max} \end{cases} \tag{14}$$

κ is the colloid deposition coefficient, which is a lumped parameter accounting for several colloid deposition mechanisms (i.e. Brownian diffusion, van der Waals forces, electric double layer forces); and $n^*_{\max}$ is the maximum deposited colloid concentration which is a function of colloidal size and the number of available sites for colloid deposition. The relationship (14) is based on the filtration theory, which has been used for the modeling of colloid deposition in porous media (e.g. Herzig et al., 1970; Harvey and Garabedian, 1991) and fractured media (Bowen and Epstein, 1979). The necessary initial and boundary conditions for the physical system considered in this study are

$$n(0,x) = 0 \tag{15}$$

$$n(t,0) = n_0 \tag{16a}$$

$$-D\frac{\partial n(t,0)}{\partial x} + Un(t,0) = Un_0 \tag{16b}$$

$$\frac{\partial n(t,\infty)}{\partial x} = 0 \tag{17}$$

where n_0 is the colloid concentration at the source. Following the work of Van Genuchten (1981), the analytical solution of Eqs. (13) and (14) subject to conditions (15), (16a), and (17) is obtained as

$$n_{cc}(t,x) = \frac{n_0}{2}\left\{\exp\left[\frac{Ux}{2D}(1-\xi)\right]\operatorname{erfc}\left[\frac{x-Ut\xi}{2(Dt)^{1/2}}\right] + \exp\left[\frac{Ux}{2D}(1+\xi)\right]\operatorname{erfc}\left[\frac{x+Ut\xi}{2(Dt)^{1/2}}\right]\right\} \tag{18}$$

where

$$\xi = \left(1+\frac{8\kappa D}{Ub^2}\right)^{1/2} \tag{19}$$

where the subscript cc indicates the use of the constant concentration upstream boundary condition (16a). Similarly, the analytical solution of Eqs. (13) and (14) subject to conditions (15), (16b), and (17) is derived to be

$$n_{cf}(t,x) = n_0\left\{\frac{1}{1+\xi}\exp\left[\frac{Ux}{2D}(1-\xi)\right]\operatorname{erfc}\left[\frac{x-Ut\xi}{2(Dt)^{1/2}}\right] + \frac{1}{1-\xi}\exp\left[\frac{Ux}{2D}(1+\xi)\right]\operatorname{erfc}\left[\frac{x+Ut\xi}{2(Dt)^{1/2}}\right] + \frac{Ub^2}{4D\kappa}\exp\left(\frac{Ux}{D}-\frac{2U\kappa t}{b^2}\right)\operatorname{erfc}\left[\frac{x+Ut}{2(Dt)^{1/2}}\right]\right\} \quad (\kappa > 0, \quad n^* < n^*_{\max}) \tag{20}$$

where the subscript cf indicates the use of the constant flux upstream boundary condition (16b). It should be noted that for the case where $n^* \geqslant n^*_{\max}$ or equivalently $\kappa = 0$, Eq. (20) can not be employed. For this case the appropriate analytical solution is given by Gershon and Nir (1969)

$$n_{cf}(t,x) = \frac{n_0}{2}\left\{\operatorname{erfc}\left[\frac{x-Ut}{2(Dt)^{1/2}}\right] + \left(\frac{4U^2t}{\pi D}\right)\exp\left[-\frac{(x-Ut)^2}{4Dt}\right] - \left(1+\frac{Ux}{D}+\frac{U^2t}{D}\right)\exp\left(\frac{Ux}{D}\right)\operatorname{erfc}\left[\frac{x+Ut}{2(Dt)^{1/2}}\right]\right\} \quad (\kappa = 0, \quad n^* \geqslant n^*_{\max}) \tag{21}$$

For a given boundary condition and the fraction of the fracture surface covered by colloids, ϵ, the appropriate mathematical expression for $n(t,x)$ (Eqs. 18, 20, or 21) is supplied to the final solution of Eq. (6). The expression for $n^*(t,x)$ is determined using Eq. (14).

4. Comparison with an analytical solution

In order to check the accuracy of the numerical solution presented, we used an already existing analytical solution for the simpler case where no colloids are present. For this special case Eq. (6) reduces to the following linear partial differential equation

$$R\frac{\partial c(t,x)}{\partial t} = D\frac{\partial^2 c(t,x)}{\partial x^2} - U\frac{\partial c(t,x)}{\partial x} - R\lambda c(t,x) + \frac{2\theta \mathscr{D}_m}{b}\frac{\partial c_m(t,x)}{\partial z}\Big|_{z=b/2} \tag{22}$$

where R is the retardation factor in the fracture defined as

$$R = 1 + \frac{2K_f}{b} \tag{23}$$

The solution of Eq. (22) coupled with Eq. (7) subject to boundary conditions (9), (10a), (11) and (12) is (Tang et al., 1981)

$$c(t,x) = \frac{c_0}{\pi^{1/2}}\int_l^\infty \exp\left(B - \zeta^2 - \frac{B^2}{4\zeta^2}\right)\left\{\exp\left(-\frac{\lambda R x^2}{4D\zeta^2} - \frac{\lambda^{1/2}Ax^2}{4\zeta^2}\right)\right.$$
$$\times \operatorname{erfc}\left[\frac{Ax^2}{8\zeta^2 T^{1/2}} - (\lambda T)^{1/2}\right] + \exp\left(-\frac{\lambda R x^2}{4D\zeta^2} + \frac{\lambda^{1/2}Ax^2}{4\zeta^2}\right)$$
$$\left.\times \operatorname{erfc}\left[\frac{Ax^2}{8\zeta^2 T^{1/2}} + (\lambda T)^{1/2}\right]\right\} d\zeta \tag{24}$$

where

$$T = \left(t - \frac{Rx^2}{4D\zeta^2}\right) \tag{25a}$$

$$A = \frac{2\theta}{bD}(R_m \mathscr{D}_m)^{1/2} \tag{25b}$$

$$B = \frac{Ux}{2D} \tag{25c}$$

$$l = \frac{x}{2}\left(\frac{R}{Dt}\right)^{1/2} \tag{25d}$$

and ζ is a dummy integration variable. A comparison between the numerical and the analytical solution for different rock-matrix retardation factors (R_m) is presented in Fig. 2(a), and for different partition coefficients for contaminant sorption on to fracture surfaces (K_f) is presented in Fig. 2(b). Very good agreement is shown between the two solutions.

5. Model simulations and discussion

To illustrate the impact of the presence of colloids on contaminant transport,

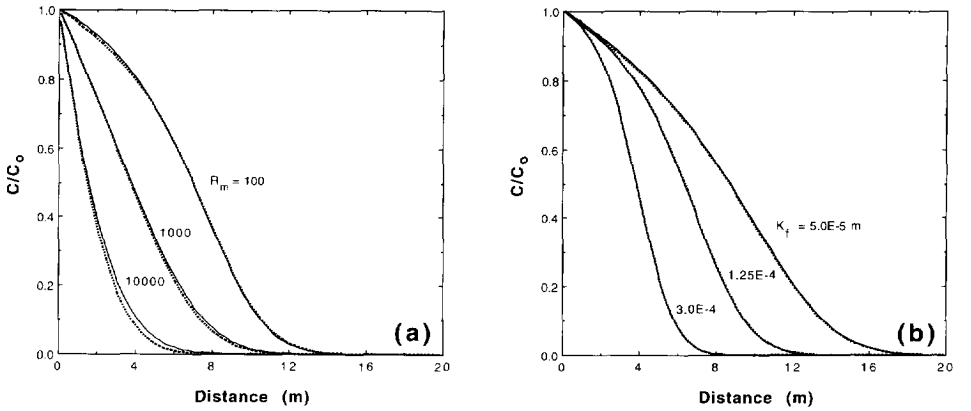

Fig. 2. Comparison of numerical and analytical solutions for the case of contaminant transport in the absence of colloids for different (a) rock-matrix retardation factors, and (b) partition coefficients for contaminant sorption on to fracture surfaces. Solid lines represent the numerical solution and broken lines represent the analytical solution.

temporal and spatial distributions of the contaminant concentration have been calculated for a variety of situations. For presentation purposes, the calculated contaminant concentrations are normalized by the source contaminant concentration. Unless otherwise specified, breakthrough curves are predicted at a distance $x = 5$ m downstream of the source, whereas snapshots are given at $t = 25y$. With the exception of K_n and K_{n^*}, the parameter values used in the simulations have been obtained from KBS-3 (1983), Abelin (1986), Skagius and Neretnieks (1986), Summers and Roberts (1988), and Toran and Palumbo (1992) and are listed in Table 1. It should be noted that the numerical values for K_n and K_{n^*} can not be compared directly, because they

Table 1
Typical parameter values for the transport model

Parameter	Value	Units
Fracture and rock matrix		
b	1.25×10^{-4}	m
D	0.25	$m^2\ year^{-1}$
$\mathscr{D}_m$	1.0×10^{-6}	$m^2\ year^{-1}$
K_f	1.0×10^{-4}	m
U	1.0	$m\ year^{-1}$
θ	0.003	
λ	1.0×10^{-6}	$year^{-1}$
ρ_b	2.0×10^{6}	$g\ m^{-3}$
Colloids		
a	0.35	
d	0.35	
K_n	2.5	$(g\ g^{-1})^{1-a}$
K_{n^*}	0.085	$(g\ g^{-1})^{1-d} m^d$
κ	1.0×10^{-10}	m

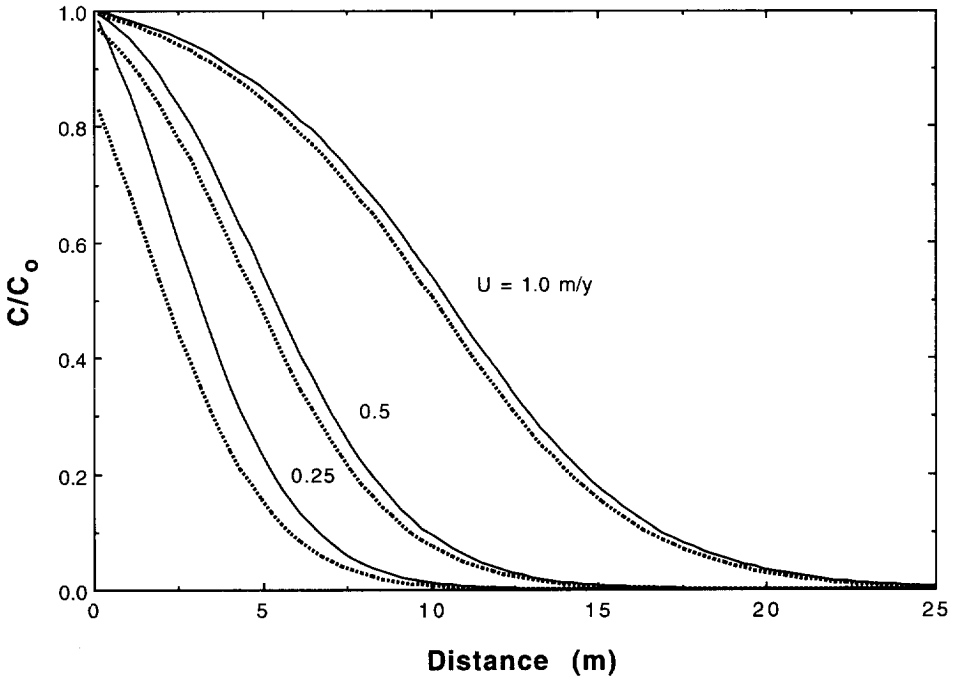

Fig. 3. Effect of inlet boundary condition on spatial normalized liquid-phase contaminant concentration distribution for different velocities. Solid lines represent the constant concentration and broken lines represent the constant flux boundary condition.

have different units. However, liquid-phase colloids are expected to be more accessible to the contaminant than deposited colloids. It has been shown that the discrepancy between the constant concentration and the constant flux boundary conditions for contaminant transport decreases with increasing velocity or equivalently decreasing dispersion (Batu and Van Genuchten, 1990). These results are also applicable to contaminant transport in the presence of colloids. Here, only the difference between the two boundary conditions for several velocities is presented (see Fig. 3).

The effects of the presence of colloids on contaminant transport are best illustrated by comparing numerical solutions using the comprehensive model (6) with the available analytical solution for the colloid-free case (24). Since the analytical solution (24) is derived for a constant concentration boundary condition (10a), all of the numerical simulations that follow are based on the same boundary condition. In Fig. 4 we have plotted the variation of the liquid-phase contaminant concentration with time and distance for different colloid deposition coefficients. The broken line represents the case where no colloids are present, while the solid lines are for different values of κ. Fig. 4(a) shows that the presence of colloids results in an earlier contaminant breakthrough. At large time and low κ the predicted concentration approaches that of the colloid-free curve (broken line); whereas, high-deposition coefficients lead to greater

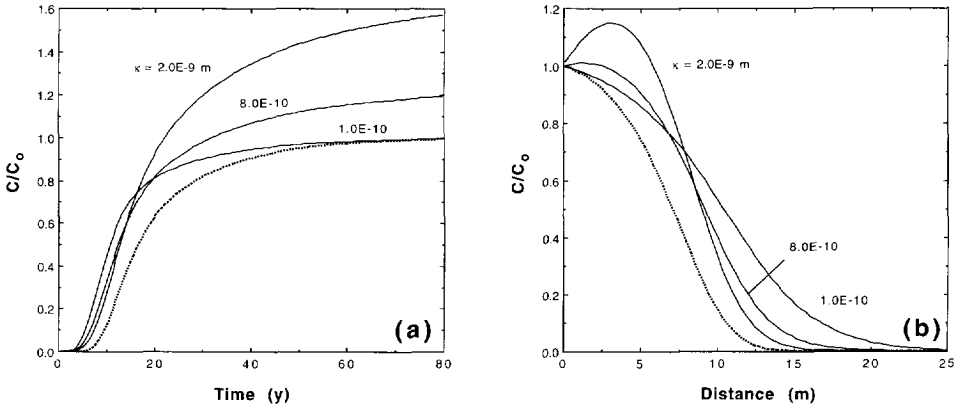

Fig. 4. Effect of colloid deposition coefficient on (a) temporal, and (b) spatial normalized liquid-phase contaminant concentration distributions. Broken lines represent the colloid-free case.

than one relative concentrations. This result is in agreement with the different but related work by Enfield et al. (1989), and Corapcioglu and Jiang (1993). An increase in κ leads to an increase in the deposited colloid concentration (see Eq. 14), and consequently a decrease in the liquid-phase colloid concentration. Therefore, the higher than one relative contaminant concentrations with increased deposited colloid concentrations is attributed to contaminant desorption imposed by the equilibrium modified Freundlich isotherm for contaminant sorption on to deposited colloids (an increase in n^* leads to a decrease in s^* and consequently an increase in c, see Eq. 4). From Fig. 4(b) it is evident that the distance traveled by colloids increases with decreasing κ (or equivalently increasing concentration of suspended colloids). Clearly, for the parameter values chosen in these simulations, colloids facilitate contaminant transport and contaminant mobility increases with increasing suspended colloid concentration.

The effect of the partition coefficient for contaminant sorption on to suspended colloids on liquid-phase contaminant concentration distribution is shown in Fig. 5(a). The predicted spatial contaminant concentration distributions indicate that increasing K_n results in an increasing liquid-phase contaminant concentration and consequently in a greater mobility of the contaminant. This is because the higher the K_n value the greater the adsorbed amount of contaminant on to suspended colloids. In view of the Freundlich isotherm (3), at certain situations when colloids enter a zone where contaminant liquid-phase concentration is not in equilibrium with contaminant concentration sorbed on to suspended colloids, desorption of contaminant back to the liquid-phase occurs. Fig. 5(b) demonstrates the effect of the partition coefficient for contaminant sorption on to deposited colloids on the spatial liquid-phase contaminant distribution. An increase in contaminant mass adsorbed on to the stationary deposited colloid particles leads to a decrease in liquid-phase contaminant concentration. However, it is evident from this figure that the contaminant exhibits retardation at high K_{n^*} values.

The effect of the exponent a in the modified Freundlich isotherm (3) on the spatial

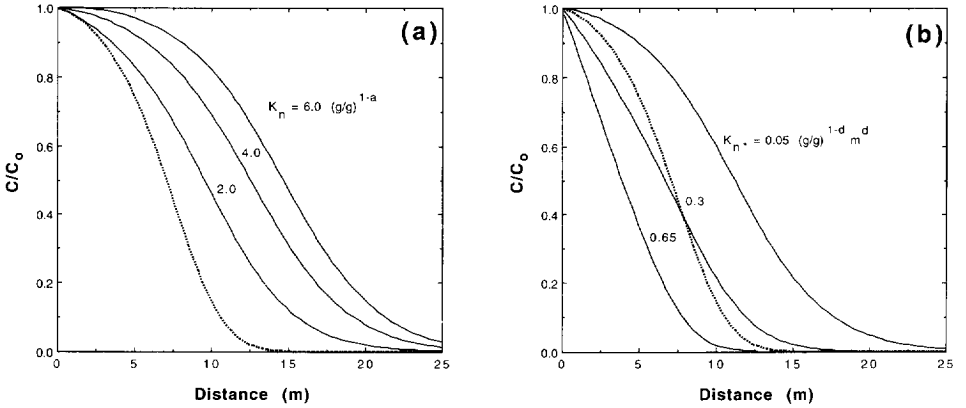

Fig. 5. Spatial normalized liquid-phase contaminant concentration distributions for different values of (a) partition coefficient for contaminant sorption on to suspended colloids, and (b) partition coefficient for contaminant sorption on to deposited colloids. Broken lines represent the colloid-free case.

liquid-phase contaminant concentration distribution is shown in Fig. 6(a); whereas, the effect of the exponent d in the Freundlich isotherm (4) is illustrated in Fig. 6(b). Higher values of the exponent a lead to higher liquid-phase contaminant concentration, while higher values of the exponent d lead to more adsorption on to deposited colloids and, consequently, lower liquid-phase contaminant concentration. Comparison of the two figures indicates that the model is much more sensitive to the exponent d. Furthermore, it is evident from Fig. 6(b) that at high d values the contaminant exhibits retardation compared with the colloid-free case.

To illustrate the effect of the initial colloid concentration n_0, simulated breakthrough curves as well as snapshots for three different ratios of initial colloid concentration to initial contaminant concentration are shown in Fig. 7. It is clearly illustrated that an increase in the initial ratio of colloid to contaminant concentration

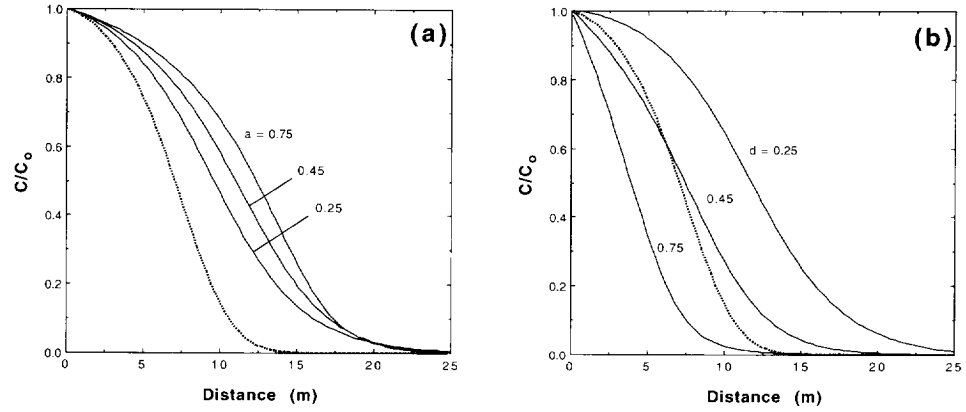

Fig. 6. Spatial normalized liquid-phase contaminant concentration distribution for different values of the modified Freundlich isotherm exponent for contaminant sorption on to (a) suspended colloids, and (b) deposited colloids. Broken lines represent the colloid-free case.

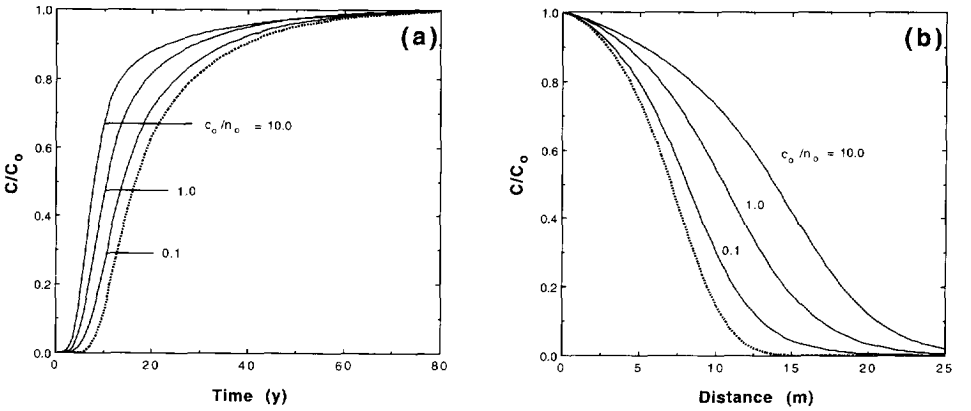

Fig. 7. The impact of colloid concentration on (a) temporal, and (b) spatial normalized liquid-phase contaminant concentration distributions. Broken lines represent the colloid-free case.

greatly enhances the contaminant transport. Fig. 8 shows the effect of the fracture aperture on the liquid-phase contaminant concentration. The extent of contaminant mobility decreases with decreasing b. This is in agreement with Eq. (14) which indicates that the rate of colloid deposition is inversely proportional to the fracture

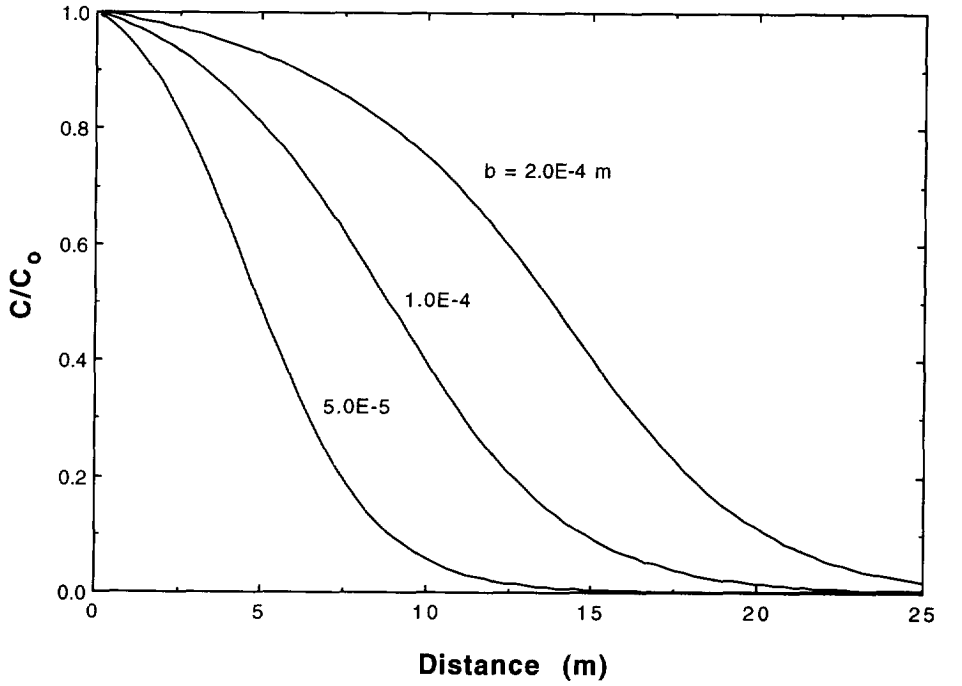

Fig. 8. Effect of fracture aperture on spatial normalized liquid-phase contaminant concentration distribution.

aperture. Moreover, matrix diffusion and sorption on to fracture surfaces and on to deposited colloids increases with decreasing fracture aperture, as the accessibility of contaminants to the rock matrix and the fracture surfaces increases. The effect of D, $\mathscr{D}_m$, R_m, and λ on liquid-phase contaminant concentration is not presented here, since it has been extensively studied for the colloid-free case (e.g. Grisak and Pickens, 1981; Tang et al., 1981; Skagius and Neretnieks, 1986; Johns and Roberts, 1991).

Fig. 9 shows the spatial distribution of the total mobile-phase contaminant concentration (liquid-phase concentration plus concentration adsorbed on to suspended colloids) normalized with the initial total contaminant concentration ($c_0 + s_0$). For comparison purposes we have also included spatial distributions for the liquid-phase contaminant concentration, the contaminant concentration adsorbed on to suspended colloids, and the suspended colloid concentration. It is evident from this figure that the contaminant mass adsorbed on to suspended colloids is a significant fraction of the total mobile-phase contaminant concentration. Furthermore, it should be noted that the distance traveled by the total mobile contaminant is greater than the distance traveled by the liquid-phase concentration.

In order to investigate the behavior of the model when n^* reaches the threshold for deposited colloid concentration, n^*_{max}, we assume that every deposited particle effectively blocks a certain area of the fracture surface from further colloid

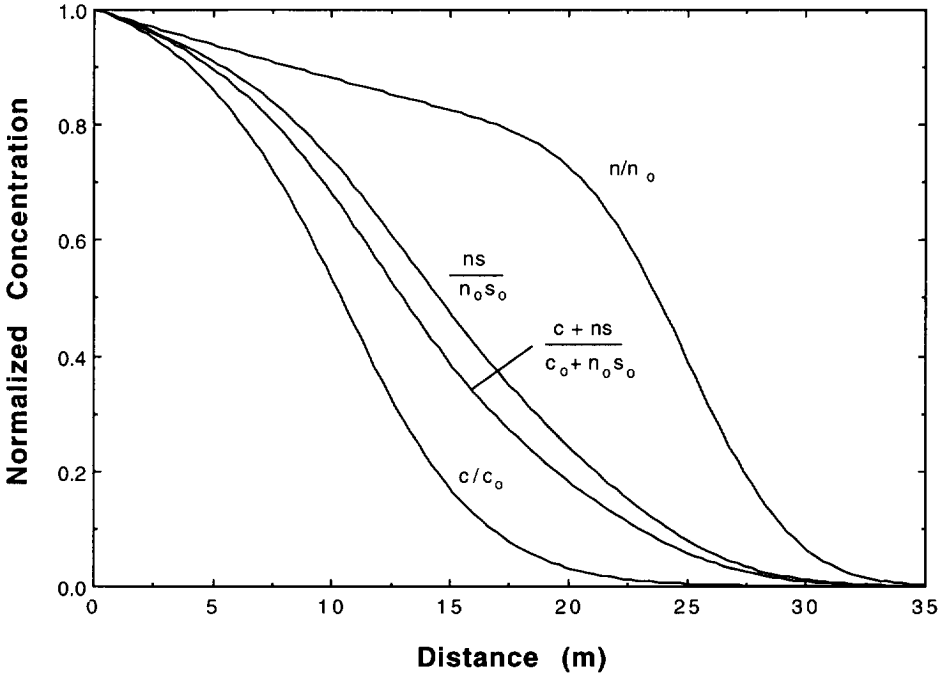

Fig. 9. Spatial normalized distributions for the liquid-phase contaminant concentration (c/c_0), the solid-phase contaminant concentration on to suspended colloids (ns/n_0s_0), the total mobile-phase contaminant concentration ($(c + ns)/(c + n_0s_0)$), and the suspended colloid concentration (n/n_0).

deposition. This assumption has also been employed by Song and Elimelech (1993) for colloid transport in porous media. The area blocked by a colloid particle is a function of colloid diameter and the number of adsorption sites on the fracture surface. Knowing the area blocked by each deposited particle, α, the maximum number of colloids, N_{max}, that could cover uniformly (i.e. square packing) a unit fracture surface area can be determined ($N_{max} = 1/\alpha$). With N_{max}, the density of particles, ρ_p, and the colloidal particle diameter, d_p, we can calculate the maximum deposited colloid concentration ($n^*_{max} = N_{max}\rho_p\pi d_p^3/6$). The deposited colloid concentration in the fracture domain is then calculated every time step and deposition is cut off from parts of the fracture where $n^* \geqslant n^*_{max}$. The calculations are made assuming spherical particles of uniform diameter of 0.02 μm with a density of 2.75 g cm^{-3} and a source colloid concentration of 100 mg l^{-1}. The fraction of the fracture surface covered by colloids, ϵ, is calculated by $\epsilon = (d_p^2/\alpha)(n^*/n^*_{max})$. It should be noted that $\epsilon = 1$ represents the case of complete monolayer coverage.

In Fig. 10 the variation of the liquid-phase contaminant concentration with time is plotted for several values of n^*_{max} with blocked fracture surface areas corresponding to α/d_p^2 of 5, 2.5, 1.67, 1.25, and 1. A rapid increase in the contaminant concentration is observed as the area blocked by each deposited particle increases. The higher the ratio of colloid size to blocked fracture surface area, the faster the increase in liquid-phase contaminant concentration. It should be noted that the simulation time for the curve

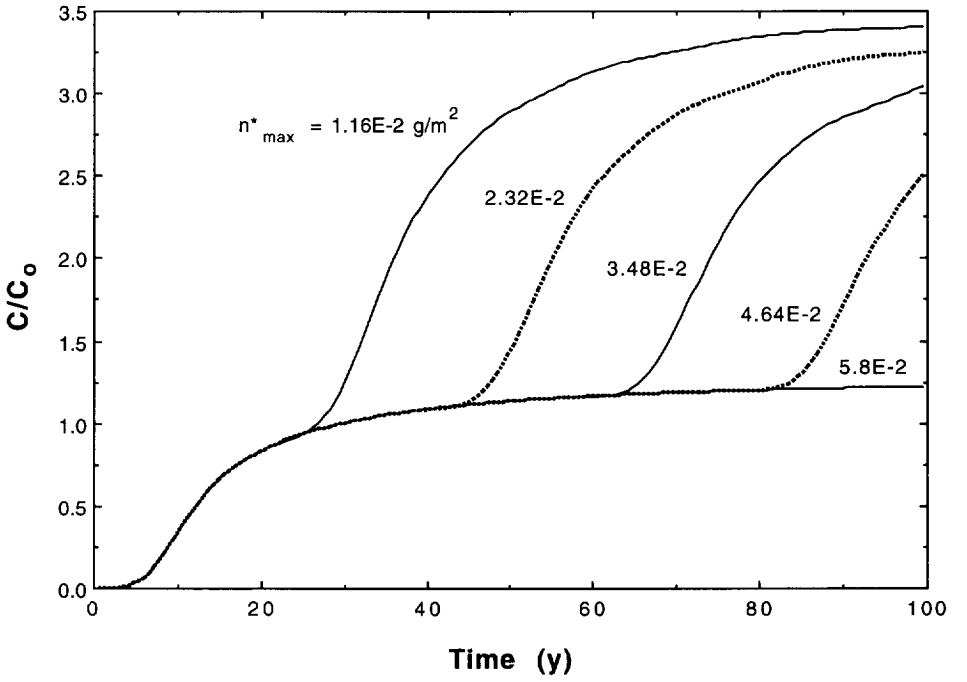

Fig. 10. Normalized liquid-phase contaminant concentration breakthrough curves for different fracture-surface capacities for colloid deposition ($\kappa = 8.0 \times 10^{-10}$ m).

corresponding to the largest n^*_{max} was not sufficiently long for the fracture surface to attain a monolayer coverage. The rapid increase in contaminant concentration after the deposited colloid concentration threshold is reached is attributed to the increase in the liquid-phase colloid concentration. Moreover, matrix diffusion and fracture sorption decrease with increasing deposited colloid concentration. The greater the deposition coefficient or the source colloid concentration, the less the time required to reach n^*_{max}.

6. Summary and conclusions

The one-dimensional contaminant transport in a single semi-infinite fracture idealized as two parallel plates is modeled accounting for reversible contaminant sorption on to fracture surfaces and on to colloids, diffusion into the rock matrix and sorption on to rock-matrix solid-surfaces, and first-order decay. Reduction in fracture sorption and matrix diffusion resulting from colloid deposition is also accounted for. It is assumed that contaminant sorption on to fracture surfaces and inside the rock matrix is governed by linear sorption isotherms; whereas, contaminant sorption on to liquid-phase and deposited colloids is governed by modified Freundlich isotherms. Analytical solutions to the partial differential equation describing the transport of colloids in a fracture assuming irreversible colloidal deposition on to fracture surfaces and no penetration into the rock matrix are used in the model solution approach. However, solutions of the comprehensive model for contaminant transport in the presence of colloids are obtained numerically by employing the fully implicit finite difference scheme for constant concentration as well as constant flux boundary conditions. For the colloid-free case and the constant concentration boundary condition, good agreement is shown between the numerical solution and an existing analytical solution.

The impact of the presence of colloids on contaminant transport is studied through parametric investigations. The liquid-phase contaminant concentration is found to be mostly sensitive to the partition coefficient for contaminant sorption on to suspended colloids. A two-fold increase in this parameter results in a substantial increase in the liquid-phase contaminant concentration. Moreover, high values of K_{n^*} and d greatly affect the mobility of the liquid-phase contaminant and can lead to contaminant retardation rather than enhancement. Also, the fracture surface capacity for colloid deposition has a great impact on the suspended colloid concentration and consequently on the contaminant transport.

References

Abelin, H., 1986. Migration in a single fracture: An in situ experiment in a natural fracture. Ph.D. Dissertation, Department of Chemical Engineering, Royal Institute of Technology, Stockholm.

Batu, V. and van Genuchten, M. T., 1990. First- and third-type boundary conditions in two-dimensional solute transport modeling. Water Resour. Res., 26(2): 339–350.

Birgersson, L. and Neretnieks, I., 1982. Diffusion in the matrix of granitic rock: field test in the Stripa mine. Part 1, SKBF/KBS Teknish Rapport, 82-08, Royal Institute of Technology, Stockholm.

Bowen, B.D. and Epstein, N., 1979. Fine particle deposition in smooth parallel-plate channels. J. Colloid Interface Sci., 72(1): 81–97.

Bradbury, M.H. and Green, A., 1986. Investigations into the factors influencing long range matrix diffusion rates and pore space accessibility at depth in granite. J. Hydrol., 89: 123–139.

Buddemeier, R.W. and Hunt, J.R., 1988. Transport of colloidal contaminants in groundwater radionuclide migration at the Nevada test site. Appl. Geochem., 3: 535–548.

Champ, D.R. and Schroeter, J., 1988. Bacterial transport in fractured rock: A field-scale tracer test at the Chalk River Nuclear Laboratories. Water Sci. Technol., 20(11/12): 81–87.

Chiou, C.T., Malcom, R.L., Brinton, T.I. and Kile, D.E., 1986. Water solubility enhancement of some organic pollutants and pesticides by dissolved humic and fulvic acids. Environ. Sci. Technol., 20(5): 502–508.

Corapcioglu, M.Y. and Haridas, A., 1985. Microbial transport in soils and groundwater: A numerical model. Adv. Water Resour., 8: 188–200.

Corapcioglu, M.Y. and Jiang, S., 1993. Colloid facilitated groundwater contaminant transport. Water Resour. Res., 29(7): 2215–2226.

De Marsily, G., 1986. Quantitative Hydrogeology: Groundwater Hydrology for Engineers. Academic, San Diego, CA.

Enfield, C.G., Bengtsson, G. and Lindqvist, R., 1989. Influence of macromolecules on chemical transport. Environ. Sci. Technol., 23(10): 1278–1286.

Gershon N.D. and Nir, A., 1969. Effects of boundary conditions of models on tracer distribution in flow through porous mediums. Water Resour. Res., 5(4): 830–839.

Grisak, G.E. and Pickens, J.F., 1981. An analytical solution for solute transport through fractured media with matrix diffusion. J. Hydrol., 52: 47–57.

Harvey R.W. and Garabedian, S.P., 1991. Use of colloid filtration theory in modeling movement of bacteria through a contaminated sandy aquifer. Environ. Sci. Technol., 25: 178–185.

Herzig, J.P., Leclerc, D.M. and Le Goff, P., 1970. Flow of suspension through porous media: Application to deep filtration. Ind. Eng. Chem., 62(5): 9–35.

Huyakorn, P.S. and Pinder, G.F., 1983. Computational Methods in Subsurface Flow. Academic, San Diego, CA.

Johns, R.A. and Roberts, P.V., 1991. A solute transport model for channelized flow in a fracture. Water Resour. Res., 27(8): 1797–1808.

Kahaner, D., Moler, C. and Nash, S., 1989. Numerical Methods and Software. Prentice Hall, New Jersey.

KBS-3, 1983. Final storage of spent nuclear fuel, 4, technical report. Swedish Nuclear Fuel Supply, Stockholm.

Krishnamoorthy, T.M., Nair, R.N. and Sarma, T.P., 1992. Migration of radionuclides from a granite repository. Water Resour. Res., 28(7): 1927–1934.

McCarthy, J.F. and Zachara, J.M., 1989. Subsurface transport of contaminants. Environ. Sci. Technol., 23(5): 496–502.

McDowell-Boyer, L.M., Hunt, J.R. and Sitar, N., 1986. Particle transport through porous media. Water Resour. Res., 22(13): 1901–1921.

McKinley, J.P. and Jenne, E.A., 1991. Experimental investigation and review of the solids concentration effect in adsorption studies. Environ. Sci. Technol., 25(12): 2082–2087.

Mills, W.B., Liu, S. and Fong, F.K., 1991. Literature review and model (COMET) for colloid/metals transport in porous media. Ground Water, 29(2): 199–208.

Moreno, L., Tsang, Y.W., Tsang, C.F., Hale, F.V. and Neretnieks, I., 1988. Flow and tracer transport in a single fracture: A stochastic model and its relation to some field observations. Water Resour. Res., 24: 2033–2048.

Moulin, V. and Ouzounian, G., 1992. Role of colloids and humic substances in the transport of radioelements through the geosphere. Appl. Geochem. Suppl., 1: 179–186.

NAGRA (Project Gewahr), 1985. Endlager fur hochaktive abfalle: sicherheitsbericht. Rep. NGB 85-05, Nat. Genossenschaft fur die Lagerung Radioaktiver Abfalle, Baden, Switzerland.

Neretnieks, I., 1983. A note on fracture flow dispersion mechanisms in the ground. Water Resour. Res., 23: 561–570.

Neretnieks, I., Eriksen, T. and Tahtinen, P., 1982. Tracer movement in a single fissure in granitic rock: Some experimental results and their interpretation. Water Resour. Res., 18: 849–858.

Neuzil, C.E. and Tracy, J.V., 1981. Flow through fractures. Water Resour. Res., 17: 191–199.

Novakowski, K.S., Evans, G.V., Lever, D.A. and Raven, K., 1985. A field example of measuring hydrodynamic dispersion in a single fracture. Water Resour. Res., 21: 1165–1174.

Press, W.H., Teukolsky, S.A., Vetterling, W.T. and Flannery, B.P., 1992. Numerical Recipes in Fortran: The Art of Scientific Computing. Cambridge University, New York, 963 pp.

Puls, R.W. and Powell, R.M., 1992. Transport of inorganic colloids through natural aquifer material: Implications for contaminant transport. Environ. Sci. Technol., 26: 614–621.

Raven, K.G., Novakowski, K.S. and Lapeciv, P.A., 1988. Interpretation of field tracer tests of a single fracture using a transient solute storage model. Water Resour. Res., 24: 2019–2032.

Shapiro, A.M. and Nicholas, J.R., 1989. Estimating the statistical properties of fracture aperture using field scale hydraulic and tracer tests: Theory and application. Water Resour. Res., 25: 817–828.

Skagius, K. and Neretnieks, I., 1986. Porosities and diffusivities of some nonsorbing species in crystalline rocks. Water Resour. Res., 22(3): 389–398.

Smith, P.A. and Degueldre, C., 1993. Colloid-facilitated transport of radionuclides through fractured media. J. Contam. Hydrol., 13: 143–166.

Song L. and Elimelech, M., 1993. Dynamics of colloid deposition in porous media: Modeling the role of retained particles. Colloids Surf., A73: 49–63.

Strikwerda, J.C., 1989. Finite Difference Schemes and Partial Differential Equations. Wadsworth & Brooks/Cole, Pacific Grove, CA.

Summers, R.S. and Roberts, P.V., 1988. Activated carbon adsorption of humic substances. J. Colloid Interface Sci., 122(2): 367–381.

Tang, D.H., Frind, E.O. and Sudicky, E.A., 1981. Contaminant transport in fractured porous media: Analytical solution for a single fracture. Water Resour. Res., 17(3): 555–564.

Toran, L. and Palumbo, A.V., 1992. Colloid transport through fractured and unfractured laboratory sand columns. J. Contam. Hydrol., 9: 289–303.

Torok, J., Buckley, L.P. and Woods, B.L., 1990. The separation of radionuclide migration by solution and particle transport in soil. J. Contam. Hydrol., 6: 185–203.

Tsang, Y.W. and Tsang, C.F., 1987. Channel model of flow through fractured media. Water Resour. Res., 23: 467–479.

Van der Lee, J., Ledoux, E. and de Marsily, G., 1992. Modeling of colloidal uranium transport in a fractured medium. J. Hydrol., 139: 135–158.

Van Genuchten, M.Th., 1981. Analytical solutions for chemical transport with simultaneous adsorption, zero-order production and first-order decay. J. Hydrol., 49: 213–233.